exposed nucleus is very active in response to the direct insolation. Because the activity will continue for many rotations, the polar region is expected to lose more material than other regions. Evidence for such erosion may be found in the depressed "broad central plain" described by Keller *et al.* (*16*) (although the limb profile shows no depression at the region of activity).

The enhanced activity at the polar region is likely to extend over the entire solar circumpolar area, with the rotation pole lying at the center of the active area. Because Giotto obtained images only from the approach direction, there are no data on the extent of the polar active zone on the other face of the nucleus. However, comparison of the observed active region with the expected circular shape of the active polar zone suggests that the pole lies near the limb of the nucleus, consistent with other values for the rotation axis. Any nutation will affect the insolation at the solar circumpolar regions, and the 7.4-day modulation of the coma activity may be related to the effects of nutation, causing the position of a source region to alternate between inside and outside the solar circumpolar zone.

REFERENCES AND NOTES

1. R. Reinhard, *Nature* **321**, 313 (1986).
2. R. Z. Sagdeev *et al.*, *ibid.*, p. 262.
3. H. J. Reitsema *et al.*, in *Proceedings of the 20th ESLAB Symposium on the Exploration of Halley's Comet*, B. Battrick, E. J. Rolfe, R. Reinhard, Eds. (Publication ESA SP-250, European Space Agency, Paris, 1986), pp. 351–354.
4. F. L. Whipple, *Astrophys. J.* **111**, 779 (1950).
5. H. U. Keller *et al.*, *Nature* **321**, 320 (1986).
6. H. J. Reitsema, W. A. Delamere, F. L. Whipple, in *Proceedings of the Symposium on the Diversity and Similarity of Comets*, E. J. Rolfe and B. Battrick, Eds. (Publication ESA SP-278, European Space Agency, Paris, 1986), pp. 455–459.
7. Z. Sekanina and S. M. Larson, *Astron. J.* **89**, 1408 (1984).
8. ———, *ibid.* **92**, 462 (1986).
9. M. J. S. Belton, P. Wehinger, S. Wychoff, H. Spinrad, in *Proceedings of the 20th ESLAB Symposium on the Exploration of Halley's Comet*, B. Battrick, E. J. Rolfe, R. Reinhard, Eds. (Publication ESA SP-250, European Space Agency, Paris, 1986), pp. 599–603.
10. R. L. Mills and D. G. Schleicher, *Nature* **324**, 646 (1986).
11. M. C. Festou *et al.*, *Astron. Astrophys.* **187**, 575 (1987).
12. A. I. F. Stewart, *ibid.*, p. 369.
13. K. Wilhelm, *Nature* **327**, 27 (1987).
14. B. A. Smith, S. M. Larson, K. Szegö, R. Z. Sagdeev, *ibid.*, **326**, 573 (1987).
15. Z. Sekanina, *ibid.* **325**, 326 (1987).
16. H. U. Keller *et al.*, *Astron. Astrophys.* **187**, 807 (1987).
17. P. R. Weismann, *ibid.*, p. 873.
18. K. Wilhelm *et al.*, in *Proceedings of the 20th ESLAB Symposium on the Exploration of Halley's Comet*, B. Battrick, E. J. Rolfe, R. Reinhard, Eds. (Publication ESA SP-250, European Space Agency, Paris, 1986), pp. 367–369.
19. This conventional definition of the rotation pole gives, for comet Halley, the north rotation pole oriented toward the ecliptic southern hemisphere. We use the ecliptic designations for cardinal directions.
20. R. Z. Sagdeev *et al.*, *Astron. Astrophys.* **187**, 835 (1987).
21. S. M. Larson, Z. Sekanina, D. Levy, S. Tapia, M. Senay, *ibid.*, p. 639.

22. We thank the Giotto and HMC teams, who were responsible for the success of the mission, and our colleagues on the HMC and Vega imaging teams for their cooperation in sharing data and results. Supported by NASA grants NASW-3573 and NSG-7082.

23 May 1988; accepted 18 October 1988

A Relation to Describe Rate-Dependent Material Failure

BARRY VOIGHT

The simple relation $\dot{\Omega}^{-\alpha}\ddot{\Omega} - A = 0$, where Ω is a measurable quantity such as strain and A and α are empirical constants, describes the behavior of materials in terminal stages of failure under conditions of approximately constant stress and temperature. Applicable to metals and alloys, ice, concrete, polymers, rock, and soil, the relation may be extended to conditions of variable and multiaxial stress and may be used to predict time to failure.

THE PREDICTION OF DEFORMATION and failure of materials from fundamental relations that are based on physically observable internal parameters (such as vacancies, crystalline structure, dislocation structure, and microcracks) can rarely be directly or easily accomplished. In practice, it is therefore necessary to consider empirical propositions, some of which nevertheless have striking if incompletely understood generality. Such a proposition for the terminal stages of rate-dependent material failure is

$$\dot{\Omega}^{-\alpha}\ddot{\Omega} - A = 0 \qquad (1)$$

where A and α are the constants of experience and Ω is an appropriate measurable quantity. The dot refers to differentiation with respect to time. Quantities that can be represented by Ω include strains for deforming alloys, metals, polymers, concrete, soil, rock, or ice. Fields of potential application of Eq. 1 include materials science, various branches of engineering, and the earth sciences. Although the question needs to be explored further, Eq. 1 may also apply (at least approximately) to predominantly rate-independent applications, such as some cases of fatigue (rate-independent repeated loading).

Additional relations may be deduced from Eq. 1, valid for several different groups of observables. Such equivalent cases include numerous independently discovered empirical or quasi-deterministic equations that describe time-deformation relations of creep to failure, and to a certain extent such cases provide validation for the basic proposition. The equation can also be used in the forecasting of specific new phenomena and in the solution of practical problems such as failure prediction. Such matters may be of importance to public safety; for example, at Vaiont, Italy, thousands died in a flood wave induced by the failure of a reservoir slope that could have been anticipated by Eq. 1 (*1*). Other potential applications include the failure of structural components, volcanic eruption forecasting, and the prediction of earthquakes (*2*).

Equation 1 is derived from experimental

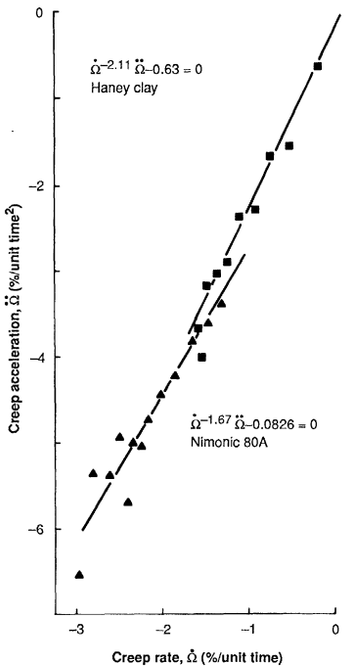

Fig. 1. The relation between creep acceleration ($\ddot{\Omega}$) and creep velocity ($\dot{\Omega}$) in terminal stages of creep of an alloy (Nimonic 80A) in tension and a soil (Haney clay) in compression (*5, 6*). Unit time is hours for Nimonic 80A and minutes for Haney clay.

College of Earth and Mineral Sciences, Pennsylvania State University, University Park, PA 16802.

observations of a linear relation between the logarithms of first and second derivatives of Ω. Insofar as I am aware, this correlation was first noted by the Japanese engineer T. Fukuzono in monitoring the movement of experimental slope failures caused by monotonic load increase (*3*). Perceiving that this application represented an interesting case of a farther reaching phenomenon, Voight derived further expressions and proposed that the relation reflected a general physical law governing diverse forms of material failure for conditions of constant stress and temperature (*4*). For the expression $\Omega = \varepsilon$ = strain, for example, the final stages of failure under constant stress and temperature conditions for an alloy in tension or a soil in compression (*5, 6*) conform to proportionality between the logarithm of creep acceleration and the logarithm of creep velocity (Fig. 1).

Integrating Eq. 1 gives expressions for rate $\dot{\Omega}$. For $\alpha = 1$ and $\dot{\Omega} = \dot{\Omega}_0$ at time $t = t_0$,

$$\dot{\Omega} = \dot{\Omega}_0 \, e^{A(t-t_0)} \tag{2}$$

For $\alpha \neq 1$,

$$\dot{\Omega} = [A(1-\alpha)(t-t_0) + \dot{\Omega}_0^{1-\alpha}]^{1/(1-\alpha)} \tag{3}$$

or

$$\dot{\Omega} = [A(\alpha-1)(t_f-t) + \dot{\Omega}_f^{1-\alpha}]^{1/(1-\alpha)} \tag{4}$$

for $\alpha > 1$, where t_f is time of failure and $\dot{\Omega}_f$ is rate at failure.

Expressions for Ω arise from double integration of Eq. 1. For example, for $\alpha > 1$, $\alpha \neq 2$, from Eq. 4,

$$\Omega - \Omega_0 = \frac{1}{A(\alpha-2)}\{[A(\alpha-1)(t_f-t_0) + \dot{\Omega}_f^{1-\alpha}]^{(2-\alpha)/(1-\alpha)} - [A(\alpha-1)(t_f-t) + \dot{\Omega}_f^{1-\alpha}]^{(2-\alpha)/(1-\alpha)}\} \tag{5}$$

Such equations can be normalized by the product of initial rate and rupture life, $\dot{\Omega}_0 t_f$. For $\alpha > 1$, $\alpha \neq 2$, and $\dot{\Omega}_f$ assumed to be infinite, a simplified form is recovered:

$$\lambda^* = \frac{\Omega}{\dot{\Omega}_0 t_f} = \frac{\alpha-1}{\alpha-2} \times [1 - (1 - t/t_f)^{(\alpha-2)/(\alpha-1)}] = \lambda[1 - (1 - t/t_f)^{1/\lambda}] \tag{6}$$

where λ^* and λ are introduced for convenience (*7*); $\lambda = (\alpha-1)/(\alpha-2)$.

At any arbitrary $t = t_*$, where $\dot{\Omega} = \dot{\Omega}_*$, t_f can be calculated by manipulation of Eq. 4:

$$t_f - t_* = \frac{\dot{\Omega}_*^{1-\alpha} - \dot{\Omega}_f^{1-\alpha}}{A(\alpha-1)} \tag{7}$$

With the approximation $\dot{\Omega}_f$ assumed to be infinite,

$$t_f - t_* = \dot{\Omega}_*^{1-\alpha}/A(\alpha-1) \tag{8}$$

gives an upper bound (but frequently useful) solution. For the common case $\alpha = 2$, further simplification arises:

$$t_f - t_* = 1/A\dot{\Omega}_* \tag{9}$$

One may estimate values of A and α from a plot such as Fig. 1 or from solving a set of simultaneous equations such as Eq. 3, using rates observed to the current time. At least four observations of Ω are generally necessary, yielding three rates. More points improve the quality of the solution, and confidence estimates may be evaluated through nonlinear statistical regression techniques. Of course, such "constants" apply strictly to the time increments over which observations have been collected and may not necessarily apply to data at subsequent times if changes occur in the dominant mechanism of deformation or in the conditions of loading. Such "constants" may therefore appear to change over time. Although the predictive method indicated here will often provide a useful guideline to the expected life, the accuracy of the method is ultimately determined by the precision and frequency of the observations and by the regularity of the observed phenomena.

One may also determine failure life graphically, using a curve of reciprocal rate against time. The reciprocal rate

$$\dot{\Omega}^{-1} = [A(1-\alpha)(t-t_0) + \dot{\Omega}_0^{1-\alpha}]^{1/(\alpha-1)} \tag{10}$$

decreases continuously with time and is upwardly convex for $\alpha > 2$ and concave for $\alpha < 2$. Experience suggests that α is frequently nearly 2, and for such cases the inverse curve is nearly linear (*3*). Failure occurs when the inverse value $\dot{\Omega}_f^{-1}$ is obtained, usually very near the point of intersection of the reciprocal rate curve with the time axis. In practice, changes in mechanism or loading conditions may cause recognizable changes in the reciprocal rate curve. Nevertheless, this method may be applied even when such complications are present. Other useful graphical relations include the logarithm of rate against the logarithm of time preceding failure, and, for $\alpha = 1$, the natural logarithm of rate against time.

Small changes in stress may have a considerable influence on t_f. This influence may be explored by considering constant load uniaxial creep tests, which comprise most of the available creep data. In the lower stress levels that characterize engineering practice, failure is associated with material damage and strains are relatively small. Under such circumstances the stress changes due to change in cross-sectional area may be neglected. The minimum creep rate $\dot{\varepsilon}_s$ corresponding to a given nominal stress σ can be expressed in the form

$$\dot{\varepsilon}_s/\dot{\varepsilon}_* = (\sigma/\sigma_*)^m \tag{11}$$

where $\dot{\varepsilon}_*$ is the minimum rate attached to an arbitrary stress σ_* and m is an experimental constant (*8*). Equations 2 through 4 and derivative expressions may be accordingly adjusted for changes in stress; for example, from Eq. 3, for $\alpha \neq 1$:

$$\dot{\varepsilon} = \{A(1-\alpha)(t-t_0) + [\dot{\varepsilon}_*(\sigma/\sigma_*)^m]^{1-\alpha}\}^{1/(1-\alpha)} \tag{12}$$

Similarly, Eq. 6 may be rewritten

Table 1. Estimates of experimental constants.

System	Number of data	m"*	α	λ	Temperature range (K)	References
			Alloys and metals			
Aluminum	150	0.85	1.85	−5.7	530–870	(*13*)
Monel	60	0.92	1.92	−11	640–1200	(*13*)
Titanium 75A; iodide titanium	100	0.87	1.87	−6.7	640–1370	(*13*)
Ferritic steels	350	0.85	1.85	−5.7	700–980	(*13*)
Austenitic steels	1000	0.93	1.93	−13	810–1090	(*13*)
Mg (2% Be)	68	0.74	1.74	−2.8	525–725	(*15*)
Zr (Fe, Cu, V, 0.4% Mo)	28	1.01	2.01	100	700–800	(*15*)
Zr (Fe, Cr, V, 0.7% Mo)	21	0.97	1.97	−32	700–800	(*15*)
Ni (6.2% Al)	42	0.91	1.91	−10	873–973	B. Voight analysis, figure 2 of (*15*)
	39	0.95	1.95	−19	1023–1073	
			Soils			
Mixed mineral soils	46	0.9	1.9	−11	Room	(*18*)
Haney clay (undisturbed)						
Isotropic triaxial	8	1.11	2.11	10	Room	(*5*)
K_0 triaxial†	7	1.09	2.09	12		
K_0 plane strain†	7	1.07	2.07	15		

*Slope of the Monkman-Grant relation. †K_0 in soil mechanics is the ratio of horizontal to vertical effective stresses during sample consolidation prior to creep loading; for the tests considered, $K_0 = 0.55$ (*5*).

$$\lambda^* = \frac{\varepsilon}{\dot{\varepsilon}_s t_f} = \frac{\alpha - 1}{\alpha - 2} \times$$
$$[1 - (1 - t/t_f)^{(\alpha-2)/(\alpha-1)}] =$$
$$\lambda[1 - (1 - t/t_f)^{1/\lambda}] \quad (13)$$

with $\dot{\varepsilon}_s = \dot{\varepsilon}_*(\sigma/\sigma_*)^m$. For variable stress histories, failure life may then be approximated by a life fraction rule of the type

$$\sum(t_i/t_f^i) = 1 \quad (14)$$

where t_i is the time over which σ_i is applied and t_f^i is the rupture time corresponding to the constant stress σ_i (*9*).

Next I consider several established relations to describe failure life that are encompassed by Eq. 1. The first case involves the Rabotnov approach to the Kachanov relations, $\dot{\varepsilon} = f(\sigma, \omega)$ and $\dot{\omega} = g(\alpha, \omega)$, where f and g are functions and ω is a dimensionless state variable, regarded in some sense as a measure of material deterioration (*10*).

For uniaxial tests the growth laws have as their simplest form

$$\dot{\varepsilon}/\dot{\varepsilon}_* = (\sigma/\sigma_*)^m(1 - \omega)^{-q} \quad (15)$$
$$\dot{\omega}/\dot{\omega}_* = (\sigma/\sigma_*)^\nu(1 - \omega)^{-r} \quad (16)$$

where m, q, ν, r, $\dot{\omega}_*$, $\dot{\varepsilon}_*$, and σ_* are material constants (*11*). For $\lambda = (r + 1)/(r - q + 1)$, the integrated form coincides with the simplified form (Eq. 13) derived from Eq. 1, for $\dot{\Omega}_0 = \dot{\varepsilon}_s$ and $\lambda = (\alpha - 1)/(\alpha - 2)$. These Rabotnov-Kachanov equations are thus exactly equivalent to this special case, for $\alpha \neq 2$ and for $\dot{\Omega}_f^{1-\alpha}$ assumed sufficiently small to be justifiably neglected.

Experimental results suggest that for steady conditions the effective strain rate may be dependent on the effective stress $\bar{\sigma}$, and the rate components $\dot{\varepsilon}_{ij}$ may be proportional to components of the stress deviator S_{ij} (*12*). If, in the tertiary region of increased rates, the ratio of strain components remains approximately constant, the Rabotnov-Kachanov equation may be generalized for multiaxial states of stress (*11*). These equations also apply to Eq. 1 as a special case. Such equations do not account for anisotropy that may accompany significant development of cracking or porosity.

The second special case involves the relation between t_f and $\dot{\varepsilon}_s$, known for decades and most frequently described by the Monkman-Grant equation (*13*),

$$t_f\,\dot{\varepsilon}_s^{m''} = C \quad (17)$$

where C is a constant. This is replicated by setting $\Omega = \varepsilon$, setting $\dot{\varepsilon} = \dot{\varepsilon}_s$ at $t = t_0 = 0$, and neglecting $\dot{\Omega}_f^{1-\alpha}$, giving from Eq. 4

$$_{tf}\,\dot{\varepsilon}_s^{\alpha-1} = 1/A(\alpha - 1) \quad (18)$$

The Monkman-Grant expression is therefore equivalent to Eq. 1 for $\dot{\Omega}_f$ large and $\alpha > 1$, where $\alpha = m'' + 1$ and $A = 1/C(\alpha - 1)$. Because Monkman-Grant type plots typically use total rupture life rather than time in tertiary creep (*13–15*), an adjustment in the time scale may be necessary for the calculation of equivalent constants. Slope changes seem minor in the few cases examined.

In the third special case, the general empirical Saito expression (*16*),

$$\dot{\varepsilon} = E\,(t_f - t)^{-n} \quad (19)$$

may be recognized as equivalent to Eq. 4, such that $E = [A(\alpha - 1)]^{1/1-\alpha}$, $n = 1/(\alpha - 1) = 1/m''$, for the case of negligible $\dot{\Omega}_f^{1-\alpha}$ and $\alpha > 1$.

The fourth case, the exponential idealization of tertiary creep, is also equivalent to Eq. 1 for $\alpha = 1$, as illustrated by Eq. 2. Additional equivalent cases have been recognized, for example, expressions of Dobeš and Milička (*15*) and Sandström and Kondyr (*17*).

Experimental data for a host of metals and alloys (*13–15*) suggest α in the range 1.74 to 2.01, with a mean value about 1.9 (Table 1). Data for various soils (*5, 16, 18*) typically suggest $\alpha = 1.9$ to 2.1. Although confidence limits are thus far poorly understood, the value of α appears to be relatively constant for a given material, independent of consolidation conditions, load level, or type of loading. Such "constants" may, however, vary over time if dominant microstructural mechanisms of deformation change, as by aging (precipitate growth), microcracking, or change in flow mechanism. The effects of such changes are roughly accumulated in m'', the Monkman-Grant exponent of Eq. 17, upon which is based much of Table 1; but such effects would appear in different proportions for observations at different times. Indeed, in some cases, mechanisms of tertiary creep may commence almost with the inception of loading; in such cases the mathematical relations of tertiary creep may require that primary creep be simultaneously analyzed.

Carefully monitored experimental slope failures in loam and sand (*2*), induced by artificial precipitation on slopes of 30° to 40° (representing effective stress increase rather than constant stress), suggest $\alpha = 2.0$ to 2.2. Natural landslides (full-scale field shear tests) analyzed by Voight commonly gave α nearly 2, as did various line length changes and tilt measurements about an expanding volcanic dome (*4*). Values of $\alpha \neq 2$ also occur. For example, slope failures analyzed by Voight encompassed the range $1 \leqq \alpha < 3$, and tertiary creep compression of ice and frozen sand gave $\alpha = 1$ (*19*).

Nevertheless, for a variety of materials characterized by diverse microstructural processes (*20*), α frequently approaches the value 2, under both laboratory and field conditions. This is important to theory because the term $\alpha - 1$ appears often as an exponent or as a multiplier in equations derived from Eq. 1, and the relations simplify for $\alpha = 2$. Often, at least, there may be only one free parameter in Eq. 1.

Some insight into $\alpha = 2$ may be gained by rearranging Eq. 1 as follows:

$$\ddot{\Omega} - A\dot{\Omega}^\alpha = 0 \quad (20)$$

If A and α are constants, then either $\alpha = 2$ or A contains time units necessary for dimensional homogeneity. The tendency of α toward 2 may imply some underlying fundamental principle. Following suggestions of an anonymous reviewer, I now explore further illustrations and some limitations regarding a specimen subjected to constant load P and (unlike previous examples) affected by reduction in cross-sectional area F, from an initial area F_0. From incompressibility (a reasonable approximation), $F = F_0 \exp(-\bar{\varepsilon})$, where natural strain $\bar{\varepsilon} = \int -dF/F$. True stress σ is related to the nominal stress σ_0 by $\sigma = P/F = \sigma_0 \exp(\bar{\varepsilon})$.

Applying the Norton relation (Eq. 11), we have

$$\dot{\bar{\varepsilon}} = \dot{\bar{\varepsilon}}_* \left(\frac{\sigma_0 e^{\bar{\varepsilon}}}{\sigma_*}\right)^m = \dot{\bar{\varepsilon}}_0\, e^{m\bar{\varepsilon}} \quad (21)$$

where $\dot{\bar{\varepsilon}}_0$ is the rate before area reduction. Differentiation gives

$$\ddot{\bar{\varepsilon}} - m\,\dot{\bar{\varepsilon}}^2 = 0 \quad (22)$$

which coincides with Eq. 1 for $\Omega = \bar{\varepsilon}$, $A = m$, and $\alpha = 2$. If, however, the nominal extension $\varepsilon = e^{\bar{\varepsilon}} - 1$ is used for the above case, the form is changed through change of variable. It therefore appears that choice of a dimensionless variable for Ω is not itself sufficient to ensure the form of Eq. 1. Likewise, setting $\Omega = F$ yields a differential equation different in form from Eq. 1.

Further, for the case of constant load rate $\dot{P}$, Eq. 11 gives

$$\dot{\bar{\varepsilon}} = -\dot{\bar{\varepsilon}}_* \left(\frac{t\,\dot{P}}{F\sigma_*}\right)^m \quad (23)$$

$$\ddot{\bar{\varepsilon}} - \frac{m}{t}\,\dot{\bar{\varepsilon}}\,(1 + t\dot{\bar{\varepsilon}}) = 0 \quad (24)$$

the latter not identical to Eq. 1. However, for large time (not necessarily implying large strain), $t\dot{\bar{\varepsilon}} \gg 1$, and the form of Eq. 1 (Eq. 22) is recovered.

A new relation (Eq. 1) thus summarizes concisely a directly observed regularity. Numerous data from many sources conform to the relation. Numerous separate long-standing relations then emerge as equivalent cases, and one obtains insight into some limita-

tions and extensions of these relations (*21*). Equation 1 offers some practical advantages, including provision for finite values of strain, strain rate, and strain acceleration at failure, as well as simplicity and ease of manipulation. Theory permits the deduction of time of failure, which may be applied in the interest of public safety.

REFERENCES AND NOTES

1. B. Voight and C. Faust, *Geotechnique* **32**, 43 (1982); B. Voight *et al.*, in *Proceedings of the International Symposium on Engineering Geology Related to Study, Preservation, and Protection of Ancient Works, Monuments, and Historical Sites* (International Association of Engineering Geology, Athens, in press), vol. 1. Although loading conditions were not constant at Vaiont (the reservoir adjacent to the failing slope had been raised, then twice lowered and raised again, and heavy rainfall had occurred), such load variations were less extreme in the weeks preceding ultimate collapse. In any case, failure could have been predicted over a week in advance by use of the analytical (say, Eq. 8) or graphical techniques presented here, a lead time sufficient to permit evacuation of communities at risk.
2. Earthquake instability models indicate that accelerating fault slip occurs at depth before instability, and is large enough to cause measurable rate changes in lengthening trilateration lines and creepmeter surveys [W. D. Stuart, *J. Geophys. Res.* **91**, 13771 (1986)]. The precursory interval is a fraction (perhaps 1 to 6%) of the loading or recurrence time. Thus measurable geodetic or precursory seismic rate changes could occur a few years or less before large and great earthquakes ($M = 7$ to 8), and such data could be evaluated by Eq. 1.
3. T. Fukuzono, in *Proceedings of the Fourth International Conference and Field Workshop on Landslides* (National Research Center for Disaster Prevention, Tokyo, 1985), pp 145–150.
4. B. Voight, *Eos* **68**, 1551 (1987); *ibid.*, p. 1286.
5. R. G. Campanella and Y. P. Vaid, *Can. Geotech. J.* **11**, 1 (1974).
6. B. F. Dyson and D. McLean, *Met. Sci.* **2**, 37 (1977).
7. The value of the dimensionless ratio $\Omega/\dot{\Omega}_0 t_f$ at failure is λ_f^*. Where Ω = strain, λ_f^* takes on the physical significance of ductility [I. N. Goodall, R. D. H. Cockroft, E. J. Chubb, *Int. J. Mech. Sci.* **17**, 351 (1975)]. For Eq. 6, $\alpha > 2$, $t = t_f$, one recovers $\lambda = \lambda_f^*$ and thus may obtain λ and α from a measurement of strain at failure [F. A. Leckie and D. R. Hayhurst, *Proc. R. Soc. London* **340**, 323 (1974)]. Values for α may likewise be determined from observed strain-time or rate-time relations. The equality $\lambda = \lambda_f^*$ holds only for $\alpha > 2$ and only for the simplified case in which $\dot{\Omega}_f$ is neglected. For $\alpha < 2$, λ is negative and $\lambda \neq \lambda_f^*$, although Eq. 6 nevertheless provides the appropriate form of the dimensionless curve, owing to contributions by the negative exponent $1/\lambda$. For $\alpha < 2$, Eq. 6 implies theoretical $\dot{\Omega}_f \rightarrow \infty$ and $\lambda^* \rightarrow \infty$ as $t \rightarrow t_f$. Obviously physically impossible, this is the consequence of neglect of $\dot{\Omega}_f$ in the simplified equations and may be resolved by use of the general equations.
8. F. H. Norton, *Creep of Steel at High Temperature* (McGraw-Hill, New York, 1929).
9. F. K. G. Odqvist and J. Hult, *Ark. Fys.* **19**, 379 (1961); R. K. Penny and D. L. Marriott, *Design for Creep* (McGraw-Hill, New York, 1971); F. A. Leckie and D. R. Hayhurst, *Acta Metall.* **25**, 1059 (1977). Such a rule is only approximate because the sequence of stresses can be important: early overloads may initiate cracks that accelerate failure at later decreased loads, but not conversely. (This is an example of the differing dominance of various mechanisms at different stages, which would change the "constants" A and α.)
10. Y. N. Rabotnov, *Creep Problems in Structural Members* (North-Holland, Amsterdam, 1969); L. M. Kachanov, *Izv. Akad. Nauk SSSR Otd. Tekh. Nauk* **8**, 26 (1958). The Kachanov concept of damage is widely used in applied mechanics, fitting the need for constitutive equations that represent important aspects of material behavior while retaining sufficient simplicity for mathematical manipulation. A more complete description would include microcrack shape and spatial attributes and associated distribution functions. This has been demonstrated both by experiment and by computer modeling, although the resulting equations are complex and the necessary tests difficult and time-consuming.
11. F. A. Leckie, *Philos. Trans. R. Soc. London Ser. A* **228**, 27 (1978); in *Mechanics of Engineering Materials*, C. S. Desai and R. H. Gallagher, Eds. (Wiley, New York, 1984), pp. 403–414. It is usually assumed that $\omega = 0$ when the material is undamaged and $\omega = 1$ at failure, although no precise definition of the Kachanov damage parameter ω is implied. These equations can be manipulated to predict rupture life for the situation of a uniaxial specimen subjected to constant strain rate (t_R^s), leading in the case $\nu = m$ to the expression $t_R^s/t_R = \lambda$, where t_R is rupture time under constant stress for the same minimum strain rate.
12. A. E. Johnson, J. Henderson, B. Khan, *Complex Stress, Creep Relaxation, and Fracture of Metallic Alloys* (Her Majesty's Stationery Office, Edinburgh, 1962).
13. F. C. Monkman and N. J. Grant, *Proc. Am. Soc. Test. Mat.* **56**, 593 (1956).
14. I. S. Servi and N. J. Grant, *Trans. Am. Inst. Min. Met. Eng.* **191**, 909 (1951).
15. F. Dobeš and H. Milička, *Met. Sci.* **1**, 382 (1976).
16. M. Saito, *Proc. 7th Int. Conf. Soil Mech. Found. Eng.* **2**, 677 (1969); S. Yamaguchi, *Rep. Sogu Doboku Lab.* (Tokyo) (1978), p. 14; D. J. Varnes, in *Proceedings of the 7th Southeast Asian Geotechnical Conference*, I. McFeat-Smith and P. Lumb, Eds. (Hong Kong Institution of Engineers, Hong Kong, 1983), vol. 2, pp. 107–130.
17. R. Sandström and A. Kondyr, *Proc. 3rd Int. Conf. Mech. Behav. Mater.* **2**, 275 (1980).
18. M. Saito and H. Uezawa, *Proc. 5th Int. Conf. Soil Mech. Found. Eng.* **1**, 315 (1961).
19. J. M. M. Ting, *Proc. Am. Soc. Civil Eng.* **109** [*J. Geotech. Eng.* 7], 932 (1983); Y. K. Zaretsky, B. D. Chuminev, V. I. Solomatin, *Eng. Geol. (Amsterdam)* **13**, 299 (1979).
20. A. C. F. Cocks and M. F. Ashby, *Prog. Mater. Sci.* **1**, 1 (1981); L. S. Costin, *Mech. Mater.* **4**, 149 (1985); A. Dragon and Z. Mroz, *Int. J. Eng. Sci.* **17**, 121 (1979); G. Greenwood, *Proc. Int. Cong. Met.* **2**, 91 (1973); D. Krachinovitz and G. V. Fonseca, *J. Appl. Mech.* **48**, 809 (1981); M. Lorrain and K. E. Loland, in *Fracture Mechanics in Concrete*, F. H. Wittman, Ed. (North-Holland, Amsterdam, 1983), pp. 106–111; A. R. S. Ponter and D. R. Hayhurst, Eds., *Creep in Structures* (Springer-Verlag, Berlin, 1981).
21. As a further example, a reviewer noted that an equation for primary creep, based on rate process theory for constant stress and temperature, can be written in the form $\dot{\varepsilon} = Bt^{-b}$, where B and b are constants. This may be expressed as $\dot{\varepsilon}^{-\alpha}\varepsilon = Dt^{b(\alpha-1)-1}$, where D is a derived constant. This conforms to Eq. 1 if $b(\alpha - 1) - 1 = 0$, implying for α about 2, a value for b of about unity. J. K. Mitchell, R. G. Campanella, and A. Singh [*Proc. Am. Soc. Civil Eng.* **94** (SM1), 249 (1968)] reported $0.75 < b < 1$ for tests for soils, implying that Eq. 1 may have a theoretical basis in rate process theory for primary creep.

22. I thank two anonymous reviewers for perceptive and extremely helpful comments.

14 April 1988; accepted 4 October 1988

Observation of Individual DNA Molecules Undergoing Gel Electrophoresis

STEVEN B. SMITH, PAUL K. ALDRIDGE, JAMES B. CALLIS

Individual DNA molecules undergoing agarose gel electrophoresis were viewed with the aid of a fluorescence microscope. Molecular shape and orientation were studied in both steady and pulsed electric fields. It was observed that (i) DNA macromolecules advanced lengthwise through the gel in an extended configuration, (ii) the molecules alternately contracted and lengthened as they moved, (iii) the molecules often became hooked around obstacles in a U-shape for extended periods, and (iv) the molecules displayed elasticity as they extended from both ends at once. A computer model has been developed that simulates the migration of the molecules in a rotating-field gel electrophoresis experiment.

THE ADVENT OF PULSED-FIELD GEL electrophoresis (PFGE) has allowed the separation of very large DNA fragments with relative ease (*1–3*), but the underlying molecular dynamics responsible for size separation have remained obscure. The prevalent model for describing DNA macromolecular motion, known as biased reptation (*4*), asserts that a very long DNA strand must snake its way through gel pores with one end leading and with the rest of the molecule following the same path. The path chosen by the head is assumed to be a semi-random walk, biased by the electric field force. The molecule is represented as a set of charged beads connected by freely orienting links. The gel pores are represented as a segmented tube surrounding the chain.

Deutsch (*5*) has recently published a series of computer simulations based on a new model also using a chain of beads but representing the gel as a lattice of point obstructions. Computer simulations based on these two models give different pictures of molecular motion. Unfortunately, direct experimental evidence concerning molecular orientation during electrophoresis, from fluo-

S. B. Smith, Department of Genetics SK-50, University of Washington, Seattle, WA 98195.
P. K. Aldridge and J. B. Callis, Center for Process Analytical Chemistry, Department of Chemistry BG-10, University of Washington, Seattle, WA 98195.